The dynamic mean-field density functional method and its application to the mesoscopic dynamics of quenched block copolymer melts

Fraaije, J. G. E. M.; vanVlimmeren, B. A. C.; Maurits, N. M.; Postma, M.; Evers, O. A.; Hoffmann, C.; Altevogt, P.; GoldbeckWood, G.

Published in:
Journal of Chemical Physics

DOI:
10.1063/1.473129

Publication date:
1997

The dynamic mean-field density functional method and its application to the mesoscopic dynamics of quenched block copolymer melts

J. G. E. M. Fraaije, B. A. C. van Vlimmeren, N. M. Maurits, M. Postma, O. A. Evers, C. Hoffmann, P. Altevogt, and G. Goldbeck-Wood

Citation: The Journal of Chemical Physics **106**, 4260 (1997); doi: 10.1063/1.473129
View online: https://doi.org/10.1063/1.473129
View Table of Contents: http://aip.scitation.org/toc/jcp/106/10
Published by the American Institute of Physics

The dynamic mean-field density functional method and its application to the mesoscopic dynamics of quenched block copolymer melts

J. G. E. M. Fraaije,[a] B. A. C. van Vlimmeren, N. M. Maurits, and M. Postma
Bioson Research Institute & Groningen Biomolecular Sciences and Biotechnology Institute, Department of Biophysical Chemistry, University of Groningen, Nijenborgh 4, 9747 AG Groningen, The Netherlands

O. A. Evers and C. Hoffmann[b]
BASF AG, Department of Informatics, ZX/ZC, Bau C-13, D-67056 Ludwigshafen, Germany

P. Altevogt
Technical Center Europe, Scientific & Technical Systems and Solutions (STSS), IBM EMEA Cross Industry, Vangerowstraβe. 18, D-69115 Heidelberg, Germany

G. Goldbeck-Wood
Molecular Simulations Ltd., 240/250 The Quorum, Barnwell Road, Cambridge CB5 8RE, United Kingdom

(Received 14 June 1996; accepted 5 December 1996)

In this paper we discuss a new generalized time-dependent Ginzburg-Landau theory for the numerical calculation of polymer phase separation kinetics in 3D. The thermodynamic forces are obtained by a mean-field density functional method, using a Gaussian chain as a molecular model. The method is especially aimed at describing the formation kinetics of the irregular morphologies which are typical for many industrial systems. As proof of concept we present the formation of irregular morphologies in quenched symmetric and asymmetric block copolymer melts. © *1997 American Institute of Physics.* [S0021-9606(97)50710-0]

I. INTRODUCTION

A. General

In the arena of applied soft-condensed matter physics, mesoscopic dynamics models are receiving increased attention as they form a bridge between fast molecular kinetics and slow thermodynamic relaxations of macroscale properties. The topic is of considerable importance for the understanding of many types of industrial complex liquids. In this paper we address the important class of polymer and surfactant mixtures. Eventually coarse-grained models for the slow diffusive and hydrodynamic phenomena in phase-separation dynamics may serve as a simulation tool for a new breed of mesoscale chemical engineers. A few recent references from groups working in this field are Refs. 1–3. Two modern reviews of coarse-grained dynamics models are in Refs. 4 and 5.

In line with these developments, we present in this paper a method for the numerical calculation of the phase separation dynamics of block copolymer melts in 3D, using a dynamic variant of mean-field density functional theory. The method is a modification of model **B**,[6,7] i.e., it is a generalized time-dependent Ginzburg-Landau theory for conserved order parameter. The numerical calculation involves integration of functional Langevin equations, given an implicit inverse Gaussian density functional expression for the intrinsic chemical potentials. Local nonideal interactions are included via a mean field. Mesoscopic fluctuations are introduced by the explicit inclusion of noise sources, according to the fluctuation-dissipation theorem. In the present study we neglect hydrodynamic effects and we assume incompressibility, otherwise the method is quite general, and can readily be adapted to a wide variety of industrial complex polymer and surfactant liquids.

In a previous paper[8] we discussed a first crude version of the dynamic mean-field density functional method. The paper described a few simulations of the phase separation of block copolymers melts in 2D, using a lattice chain algorithm for the calculation of intrinsic chemical potentials. Since then, we have improved two crucial technical aspects of the method considerably—the details can be found in Refs. 9 and 10. In fact, without these improvements practical simulations of phase-separation dynamics in 3D are not possible.

First of all, we have changed the chain model from ideal cubic lattice chain to ideal Gaussian chain. There is a fundamental reason why we did this. It can be shown[9] that the cubic lattice chain model leads to unphysical singularities in copolymer melt inverse structure factors in 3D. This implies a disruption of the 1-1 mapping between external potential and conjugate density field. The 1-1 mapping is crucial in the density functional method,[11] and hence cubic lattice chain models cannot be used in 3D.

Second, we discovered a simple factorization method for the numerical calculation of the noise distribution in general functional Langevin models.[10] The noise calculation is not a trivial problem since the noise must have a precise correlation, dictated by the fluctuation-dissipation theorem. The kinetic coefficients we use are not constant but given by a local exchange model. In the previous paper[8] we simply added uncorrelated noise to the intrinsic chemical potentials. The correlations of the ensuing density fluctuations did not satisfy the fluctuation-dissipation theorem.

[a]Author to whom correspondence should be addressed.
[b]Present address: CERN, PPE Division, CH-1211 Geneve 23, Switzerland.

 0021-9606/97/106(10)/4260/10/$10.00

In the present paper we discuss the basic principles of the dynamic mean-field density functional method in the improved footing. In addition we have included a full density functional derivation of the free-energy functional for inhomogeneous off-equilibrium systems. Although the final equations differ only in a few minor details from those of the previous paper, we believe that the new derivation shows more clearly where the weak and strong points of the method are. We have included as proof of concept a rerun of the same systems as in the previous paper, but now in 3D.

B. Application to block copolymer melts

The industrial importance of a good model for the dynamics of the phase transitions in copolymer melts should not be underestimated. In academia, the usual practice is to prepare structured mesophases by slowly casting from solvent, or by shearing techniques.[12] Even with these laborious techniques, sometimes taking weeks or months to complete, it is not always clear whether the mesophase structure is really in equilibrium. Remarks are made that quenching in the absence of a biasing field results in messy, irregular, nonequilibrium states with ''poorly defined morphologies.''[13]

From the point of view of equilibrium theory irregular mesophase structures are extremely difficult to characterize. Indeed, since the seminal contributions of Leibler[14] and Helfand[15–17] the standard approach is to solve a variant of Gaussian chain self-consistent-field equations for some *presupposed* defect-free mesophase structure of ideal symmetry, such as lamellar, hexagonal, bcc, gyroid, etc. The free energy is then minimized with respect to the mesophase lattice parameters. This approach, similar to the older phenomenological Landau method for calculating liquid-solid transitions,[18] leads directly to phase diagrams of the considered structures (references describing this and related self-consistent-field methods in more detail can be found in Refs. 12 and 19–26). The method is certainly elegant. Nevertheless the inherent presupposition of ideal structural symmetry implies that the method fails for the description of defect structures, since by the very nature these types of morphologies are *irregular*. Indeed, the question arises what theoretical means we have to assess defect structures; and the answer must be in the dynamic properties since the dynamics determines the formation and stability of defects. A recent review discusses theory and experiment of the dynamics of block copolymers,[27] e.g., self-diffusion, collective diffusion, and viscoelastic phenomena. It seems that only very few systematic studies of the phase transition dynamics of quenched copolymer melts exist.

Yet from an industrial perspective, even a rough description of irregular nonequilibrium states is much more desired than a detailed analysis of pure equilibrium structures. Typically, the industrial processing time of a melt is orders of magnitude shorter than the thermodynamic relaxation time and thus in many cases intermediate nonperfect states must contribute substantially if not dominate the behavior of the final macroscale material. The quenched dynamics model we study here is precisely aimed at describing the formation of the ''poorly defined morphologies.''

C. Notation

The melt has volume V and contains n Gaussian chains, each of length $N=N_A+N_B$. The bead index number is $s=1,\ldots,N$. The type of the A or B beads is indexed by I. There are two external potentials, U_A and U_B, two density fields, ρ_A and ρ_B, and two intrinsic chemical potentials, μ_A and μ_B. The double brackets notation for the density functional $\rho_I[U](\mathbf{r})$ means that ρ_I is a functional of U_A and U_B and as such a function of position in space $\mathbf{r}$. $\beta^{-1}=k_BT$.

II. THEORY

A. Thermodynamics

Imagine that on a course-grained time scale, we observe at an instant of time a collective concentration field $\rho_I^0(\mathbf{r})$ of the beads of type I; this field will serve as a reference level. On this coarse-grained time scale, there will be a certain distribution of bead positions, according to a function $\Psi(\mathbf{R}_{11},\ldots,\mathbf{R}_{nN})$, where $\mathbf{R}_{\gamma s}$ is the position of bead s from chain γ. Given the distribution Ψ we can define the collective concentration of the beads s from all chains by the average of a microscopic density operator:

$$\rho_I[\Psi](\mathbf{r})\equiv\sum_{\gamma=1}^{n}\sum_{s=1}^{N}\delta_{Is}^{K}\ \mathrm{Tr}\ \Psi\,\delta(\mathbf{r}-\mathbf{R}_{\gamma s}), \tag{1}$$

where δ_{Is}^{K} is a Kronecker function with value 1 when bead s is of type I and 0 otherwise. We assume that in the slowly relaxing liquid the interactions do not depend on the momenta, and therefore we limit the trace to the integration over coordinate space only

$$\mathrm{Tr}(\cdot)\equiv\frac{1}{n!\,\Lambda^{3nN}}\int_{V^{nN}}(\cdot)\prod_{\gamma=1}^{n}\prod_{s=1}^{N}d\mathbf{R}_{\gamma s}$$

where $n!$ accounts for the indistinguishability of the chains and Λ is a thermal wavelength

$$\Lambda=\sqrt{\frac{h^2\beta}{2\pi m}},$$

where m is the mass of a bead.[28] The normalization with Λ^{3nN} ensures that the distribution Ψ is dimensionless.

Obviously we want $\rho_I^0(\mathbf{r})=\rho_I[\Psi](\mathbf{r})$, i.e., the reference concentration $\rho_I^0(\mathbf{r})$ must be identical to $\rho_I[\Psi](\mathbf{r})$, the average of the microscopic density operator, and this puts a constraint on the distribution Ψ. On the set of distribution functions Ψ we introduce an equivalence relation by defining:

$$\Psi_1\sim\Psi_2\Leftrightarrow\rho_I[\Psi_1]=\rho_I[\Psi_2]. \tag{2}$$

All distributions Ψ leading to the same density $\rho_I^0(\mathbf{r})$ form an equivalence class $\mathscr{P}$ of distribution functions:

$$\mathscr{P}=\{\Psi(\mathbf{R}_{11},\ldots,\mathbf{R}_{nN})\,|\,\rho_I^0(\mathbf{r})=\rho_I[\Psi](\mathbf{r})\}.$$

On this set of distribution functions we define an intrinsic free-energy functional $F[\Psi]$ according to

$$F[\Psi]\equiv \mathrm{Tr}(\Psi H^{id}+\beta^{-1}\Psi\ \ln\ \Psi)+F^{nid}[\rho^0]. \tag{3}$$

The first term is the average value of the Hamiltonian for internal Gaussian chain interactions:[29,30]

$$H^{id}=\sum_{\gamma=1}^{n} H_\gamma^G, \tag{4}$$

where H_γ^G is the Gaussian chain Hamiltonian of chain γ:

$$H_\gamma^G=\frac{\beta^{-1}3}{2a^2}\sum_{s=2}^{N}(\mathbf{R}_{\gamma s}-\mathbf{R}_{\gamma,s-1})^2; \tag{5}$$

here a is the Gaussian bond length parameter. The second term in the free-energy functional stems from the Gibbs entropy of the distribution $-k_B\mathrm{Tr}\,\Psi\ln\Psi$. The third term $F^{nid}[\rho^0]$ is the mean-field nonideal contribution, given the density of the reference level ρ^0. By definition, in the mean-field approximation $F^{nid}[\rho^0]$ is independent of the particular distribution Ψ chosen from the class $\mathscr{P}$. Thus, this density functional method describes all correlations within the Gaussian chains exactly; the correlations between the chains are accounted for by the mean field.

The key thermodynamic ansatz of the dynamic density functional theory is that on a coarse-grained time scale the distribution function Ψ for each time interval is such that the free-energy functional $F[\Psi]$ is minimal. Hence, in this limit there is no memory and Ψ is *independent* of the history of the system: it is fully characterized by the instantaneous constraint $\rho_I^0(\mathbf{r})=\rho_I[\Psi](\mathbf{r})$ and the minimal free-energy criterium. The constrained minimization follows the standard procedure of density functional theory.[31,32,11,33] We introduce an auxiliary thermodynamic variable $F'[\Psi]$:

$$F'[\Psi]\equiv F[\Psi]+\sum_I\int_V U_I(\mathbf{r})[\rho_I[\Psi](\mathbf{r})-\rho_I^0(\mathbf{r})]d\mathbf{r} +\lambda[\mathrm{Tr}\ \Psi-1], \tag{6}$$

where the second term contains the external potentials $U_I(\mathbf{r})$ as Lagrange multipliers for the constraining of the density fields, and the last term has a Lagrange multiplier λ for the normalization of the distribution.

The variational condition $\delta F'/\delta\Psi=0$ leads to the optimal distribution Ψ^0

$$\Psi^0=\frac{1}{Q^{id}}\,e^{-\beta[H^{id}+\Sigma_{\gamma=1}^{n}\Sigma_{s=1}^{N}U_s(\mathbf{R}_{\gamma s})]}, \tag{7}$$

where the ideal partition functional is defined as

$$Q^{id}\equiv \mathrm{Tr}\ e^{-\beta[H^{id}+\Sigma_{\gamma=1}^{n}\Sigma_{s=1}^{N}U_s(\mathbf{R}_{\gamma s})]}, \tag{8}$$

while the constraints are obeyed according to

$$1=\mathrm{Tr}\ \Psi^0, \tag{9}$$

$$\rho_I^0(\mathbf{r})=\rho_I[\Psi^0](\mathbf{r})=\rho_I[U](\mathbf{r}), \tag{10}$$

which introduces the density functional $\rho_I[U](\mathbf{r})$. Notice that the last equality follows trivially from the fact that Ψ^0 is a functional of U.

Some time ago Mermin[11] showed that density functional relations constitute unique relations between external potentials and conjugate density fields. Here, this implies that the density functional relation $\rho_I^0(\mathbf{r})=\rho_I[U]\ (\mathbf{r})$ is a *bijective* relation between the two sets of fields $\{\rho_A^0(\mathbf{r}),\rho_B^0(\mathbf{r})\}$ and $\{U_A(\mathbf{r}),U_B(\mathbf{r})\}$. The bijectivity property is crucial for the understanding of the time integration of the functional Langevin equations, discussed in more detail below.

The distribution function of the n ideal Gaussian chains factorizes exactly, and hence the density functional can be further simplified to a single-chain density functional

$$\rho_I[U](\mathbf{r})=n\sum_{s'=1}^{N}\delta_{Is'}^K\ \mathrm{Tr}_c\psi\delta(\mathbf{r}-\mathbf{R}_{s'}), \tag{11}$$

where the trace is now limited to the integration over the coordinates of one chain

$$\mathrm{Tr}_c(\cdot)=\frac{1}{\Lambda^{3N}}\int_{V^N}(\cdot)\prod_{s=1}^{N}d\mathbf{R}_s$$

and ψ is the single-chain distribution

$$\psi\equiv\frac{1}{\Phi}\,e^{-\beta[H^G+\Sigma_{s=1}^{N}U_s(\mathbf{R}_s)]}, \tag{12}$$

where Φ is the single-chain partition function

$$\Phi\equiv\mathrm{Tr}_c e^{-\beta[H^G+\Sigma_{s=1}^{N}U_s(\mathbf{R}_s)]} \tag{13}$$

and H^G is the Gaussian chain Hamiltonian of one chain. A comment regarding the normalization of the single-chain trace Tr_c with Λ^{3N} is in place here. It is of course true that each chain has only three translational degrees of freedom, not $3N$ as would be implied by the normalization with Λ^{3N}. It is therefore appropriate to replace the normalization by a term involving the three translational degrees, combined with a normalization term for the $N-1$ Gaussian integrals. This implies the replacement

$$\Lambda^{3N}\rightarrow\Lambda^3\left(\frac{2\pi a^2}{3}\right)^{3/2(N-1)}$$

in the definition of the trace Tr_c. It must be realized that this change of normalization in no way affects the statistics of the problem.

The free energy in the constrained minimum follows from reinsertion of the optimal distribution back in the formula for the intrinsic free energy. In the constrained minimum $\rho=\rho^0$ and thus $F^{nid}[\rho]=F^{nid}[\rho^0]$. We find the result

$$F[\rho]=-\beta^{-1}n\ \ln\Phi+\beta^{-1}\ \ln\ n!-\sum_I\int U_I(\mathbf{r})\rho_I(\mathbf{r})d\mathbf{r} +F^{nid}[\rho]. \tag{14}$$

Now we introduce the model for the nonideal free-energy functional

$$\begin{aligned}F^{nid}[\rho]=\tfrac{1}{2}\int\int\ &\epsilon_{AA}(|\mathbf{r}-\mathbf{r}'|)\rho_A(\mathbf{r})\rho_A(\mathbf{r}')\\ &+\epsilon_{AB}(|\mathbf{r}-\mathbf{r}'|)\rho_A(\mathbf{r})\rho_B(\mathbf{r}')+\epsilon_{BA}(|\mathbf{r}-\mathbf{r}'|)\\ &\times\rho_B(\mathbf{r})\rho_A(\mathbf{r}')+\epsilon_{BB}(|\mathbf{r}-\mathbf{r}'|)\\ &\times\rho_B(\mathbf{r})\rho_B(\mathbf{r}')d\mathbf{r}\,d\mathbf{r}',\end{aligned} \tag{15}$$

where $\epsilon_{IJ}(|\mathbf{r}-\mathbf{r}'|)$ is a mean-field energetic interaction between beads type I at $\mathbf{r}$ and J at $\mathbf{r}'$, defined by the same Gaussian kernel as in the ideal chain Hamiltonian

$$\epsilon_{IJ}(|\mathbf{r}-\mathbf{r}'|)\equiv\epsilon_{IJ}^{0}\left(\frac{3}{2\pi a^2}\right)^{3/2} e^{-(3/2a^2)(r-r')^2}. \tag{16}$$

The Gaussian kernel is normalized: $\int_V \epsilon_{IJ}(|\mathbf{r}-\mathbf{r}'|)d\mathbf{r}=\epsilon_{IJ}^{0}$. We have introduced here explicitly a nonlocality of the nonideal interactions on a length scale of the statistical unit. This seems reasonable, since the statistical unit samples a volume $\sim a^3$. On long length scales $\gg a$, the effect of the nonlocality is negligible.

The mean-field intrinsic chemical potentials can easily be derived by functional differentiation of the free energy. They are

$$\mu_A(\mathbf{r})\equiv\frac{\delta F}{\delta\rho_A(\mathbf{r})} \tag{17}$$

$$=-U_A(\mathbf{r})+\int_V \epsilon_{AA}(|\mathbf{r}-\mathbf{r}'|)\rho_A(\mathbf{r}')$$

$$+\frac{1}{2}[\epsilon_{AB}(|\mathbf{r}-\mathbf{r}'|)+\epsilon_{BA}(|\mathbf{r}-\mathbf{r}'|)]\rho_B(\mathbf{r}')d\mathbf{r}', \tag{18}$$

$$\mu_B(\mathbf{r})\equiv\frac{\delta F}{\delta\rho_B(\mathbf{r})} \tag{19}$$

$$=-U_B(\mathbf{r})+\int_V \frac{1}{2}[\epsilon_{AB}(|\mathbf{r}-\mathbf{r}'|)+\epsilon_{BA}(|\mathbf{r}-\mathbf{r}'|)]$$

$$\times\rho_A(\mathbf{r}')+\epsilon_{BB}(|\mathbf{r}-\mathbf{r}'|)\rho_B(\mathbf{r}')d\mathbf{r}'. \tag{20}$$

In equilibrium $\mu_I(\mathbf{r})=$const, this results in the familiar self-consistent-field equations for the mean-field Gaussian chain model. In general, these equations will have many solutions, one of which will be a state of lowest free energy; most states will be metastable. We do not solve the self-consistent field equations here. Rather, when the system is not in equilibrium $-\nabla\mu_I$ is a thermodynamic force, which by the inversion of the density functional and the explicit form of the nonideal interactions is a unique functional of the density. Thus we can use the equations to set up a generalized time-dependent Ginzburg-Landau theory.

B. Dynamics

We introduce the following functional Langevin equations for the diffusive dynamics of the density fields:

$$\frac{\partial\rho_A(\mathbf{r})}{\partial t}=M\nu\nabla\cdot\rho_A\rho_B\nabla[\mu_A-\mu_B]+\eta, \tag{21}$$

$$\frac{\partial\rho_B(\mathbf{r})}{\partial t}=M\nu\nabla\cdot\rho_A\rho_B\nabla[\mu_B-\mu_A]-\eta. \tag{22}$$

The distribution of the Gaussian noise η satisfies the fluctuation-dissipation theorem:[34–36]

$$\langle\eta(\mathbf{r},t)\rangle=0, \tag{23}$$

$$\langle\eta(\mathbf{r},t)\,\eta(\mathbf{r}',t')\rangle=-2M\nu\beta^{-1}\delta(t-t')$$

$$\times\nabla_{\mathbf{r}}\cdot\delta(\mathbf{r}-\mathbf{r}')\rho_A\rho_B\nabla_{\mathbf{r}'}, \tag{24}$$

M is a bead mobility parameter. The Langevin equations are constructed for an *incompressible* system, with dynamic constraint

$$\nu^{-1}\equiv\rho_A(\mathbf{r},t)+\rho_B(\mathbf{r},t), \tag{25}$$

where ν is a constant molecular volume, i.e., the volume occupied by one statistical unit. The kinetic coefficient $M\nu\rho_A\rho_B$ models a local exchange mechanism, such that any net flux of material is zero. The exchange equations can be derived by adding an extra constraining pressure functional to the intrinsic chemical potentials, assuming that the bare kinetic coefficients are local and uncoupled (Appendix A).

The special correlation of the noise ensures that time integration of the Langevin equations generates a Boltzmann ensemble of density fields with probability distribution

$$\frac{1}{\mathcal{Q}}e^{-\beta F[\rho]}, \tag{26}$$

where $\mathcal{Q}$ is the ''grand'' partition function

$$\mathcal{Q}=\int_C e^{-\beta F[\rho]}d\{\rho_A\}d\{\rho_B\},$$

$$C=\{\{\rho_A(\mathbf{r}),\rho_B(\mathbf{r})\}\,|\,\rho_A(\mathbf{r})+\rho_B(\mathbf{r})=\nu^{-1}\}. \tag{27}$$

The grand free energy of the total system, including the fluctuations is

$$\mathcal{F}=-\beta^{-1}\ln\mathcal{Q}. \tag{28}$$

C. Numerics

The Gaussian chain density functional Eq. (11) constitutes a 1-1 relation between the external potentials U_A and U_B and the density fields ρ_A and ρ_B; according to the equations (17) and (19) the intrinsic chemical potentials μ_A and μ_B are functionals of the external potentials and the density fields; the coupled Langevin equations (21) and (22) constitute a relation between the time derivatives $\partial\rho_A/\partial t$ and $\partial\rho_B/\partial t$ and the intrinsic chemical potentials μ_A and μ_B; the equations (23) and (24) for the noise source relate the noise to the exchange kinetic coefficient. Together, these equations form a closed set. The set can be integrated efficiently on a cubic mesh by a Crank-Nicolson scheme.[37] The details of the numerics will be discussed in a following publication; a summary is given in Appendix B. From the numerical analysis is turns out that four dimensionless parameters are important:

$$\tau\equiv\beta^{-1}Mh^{-2}t, \tag{29}$$

$$d\equiv ah^{-1}, \tag{30}$$

$$\Omega\equiv\nu^{-1}h^3, \tag{31}$$

$$\chi\equiv\frac{\beta\nu^{-1}}{2}[\epsilon_{AB}^{0}+\epsilon_{BA}^{0}-\epsilon_{AA}^{0}-\epsilon_{BB}^{0}]. \tag{32}$$

The dimensionless time τ scales the time t, mesh size h, and bead diffusion coefficient $\beta^{-1}M$. The grid scaling parameter

d is introduced for the calculation of the Gaussian chain density functional by an off-lattice stencil algorithm, in which the repeated application of the Gaussian kernel $e^{-(3/2a^2)(\mathbf{r}-\mathbf{r}')^2}$ is replaced by a local grid-restricted convolution operator (Appendix B). χ is the familiar interaction exchange parameter.

A special parameter is Ω, this is the constant total number of beads in each cell [since in the incompressible system $\Omega=\nu^{-1}h^3=(\rho_A+\rho_B)h^3$]. The variance of the dimensionless noise scales with $\Delta\tau/\Omega$ ($\Delta\tau$ is the time step) so that the higher Ω, i.e., the more beads in each cell, the lower the influence of the noise. This can be understood quite intuitively: if there are many beads in a cell, then the fluctuation in the relative concentration of one of the bead types $|\delta\rho_I/(\rho_A+\rho_B)|=|\delta\nu\rho_I|$ in that cell must be small. If there are only a few beads, then the relative fluctuation must be large. In fact, Ω can be interpreted as a so-called size-expansion parameter.[36] The Langevin model for the dynamics can only hold in the limit where there is sufficient statistical averaging in each cell. If the value of Ω is chosen too small ($\Omega\approx1$) the dynamics model is not realistic.

III. RESULTS AND DISCUSSION

A. Irregular morphologies

In Figs. 1 and 2 the time-dependent morphologies of two copolymer melts are depicted: A_8B_8 (Fig. 1) and A_6B_{10} (Fig. 2). In Fig. 3 is depicted the time evolution of a volume-averaged order parameter $\overline{p^2}$, defined by

$$\overline{p^2}\equiv\frac{1}{2}+\frac{\nu^2}{V}\int(\rho_A-\rho_B)^2d\mathbf{r}. \tag{33}$$

Here the local order parameter is $\nu(\rho_A-\rho_B)$.

The numerical parameters for the simulations are: $\Delta\tau=0.5$, $d=1.154\,30$ (the optimal value, see Appendix B), $\Omega=100$ and $\chi=1.0$. The seed for the random number generator was identical for both simulations. In both cases the melts were equilibrated for 100 time steps at $\chi=0$, prior to the quench to $\chi=1.0$ at time $\tau=50$. In the absence of fluctuations the spinodal values are $\chi_s=0.79$ (A_8B_8) and $\chi_s=0.90$ (A_6B_{10}). The relaxation of the athermal melt from homogeneous state ($\rho_I=$const) to fluctuation equilibrium takes only a few units of time. On the scale of Fig. 3 the initial start-up is practically instantaneous. Notice further that on this scale the time evolution of $\overline{p^2}$ is fairly smooth.

In both cases we see clearly that the quenched phase separation indeed leads to the rapid development of irregular ordered states, in agreement with experimental findings. In the symmetric melt (Fig. 1) a messy lamellar phase develops, full of defects. Close inspection of the fluctuation equilibrated athermal melt, directly before the quench, shows the constant formation and annihilation of disordered correlation holes, due to the thermal excitations. After the quench the first degree of organization is a rapid rearrangement of the holes in some irregular superlattice. This irregular superlattice is partly conserved in the defect structure of the ordered state.

From the isosurface representation [Fig. 1(d)] it is tentative to denote these structures as bicontinuous. From visual inspection it is obvious that we can trace a path from any side of the box to any other side of the box, through one single phase. So there is at least one structure which percolates the system, and since the melt is symmetric, both phases must have percolating structures. However, a representation at a higher isosurface level shows also smaller, trapped structures which are disconnected and do not percolate. This shows the difficulty of assigning the qualifier bicontinuity to random field systems, since the measures ''connected'' or ''disconnected'' depend on the chosen density levels for the isosurfaces.

Given these reservations, the final morphology in the asymmetric melt [Fig. 2(d)] is also bicontinuous, but now the basic structural elements are cylinders. The cylinders are certainly not perfect. In many cases branches and intertwining can be seen. Whether they are all connected or not depends again on the isosurface level. In view of the large number of defects it seems difficult to assign an ideal type to the ordered phase. There are, however, a number of three-handle connections between cylinders, and therefore this may perhaps be classified as a defected gyroid phase (we thank G. Fredrickson for pointing this out to us).

In the previous paper[8] the simulations were limited to 2D. There are many properties which are qualitatively different in the present 3D simulation. Obviously, in 2D there is no bicontinuity, and yet this effect seems important in 3D. Also, the ordered state in the 2D asymmetric melts showed a hexagonal array of dots, whereas in 3D the structural elements are cylinders. Despite these qualitative differences the major conclusion regarding the quench experiment remains unaltered: the spatial organization of isotropic correlation holes is partly frozen in the defect structure of the ordered state.

B. The noise factor

The values $\Omega=100$ and $N=16$ apply to short polymers with rather long statistical units and a relatively small molecular volume. Since $d=a/h$ and $\Omega=h^3/\nu$ we have

$$\frac{\nu}{a^3}=\frac{1}{\Omega d^3}. \tag{34}$$

Inserting the values $\Omega=100$ and $d=1.1543$ we find $\nu/a^3\approx6.5\times10^{-3}$. It is illustrative to compare this ratio with experimental values. A recent review[38] contains a large number of data relating to the structure/chain-flexibility relationships of polymers. From the data it seems that Flory's characteristic ratio C_∞ is usually between 5 and 15.[38] If we identify the Gaussian bond length a with the Kuhn length, then we can estimate a from $a=(C_\infty+1)l$,[38] where l is the length of the chemical monomer unit. Hence, in this model the Gaussian bead represents a string of $C_\infty+1$ monomer units, each of size l. If, for sake of argument, we further assume that the volume of each monomer is $\approx l^3$ then it follows that $\nu/a^3\approx(C_\infty+1)l^3/(C_\infty+1)^3l^3=1/(C_\infty+1)^2$, which is between 4×10^{-3} and 3×10^{-2}. Much more precise

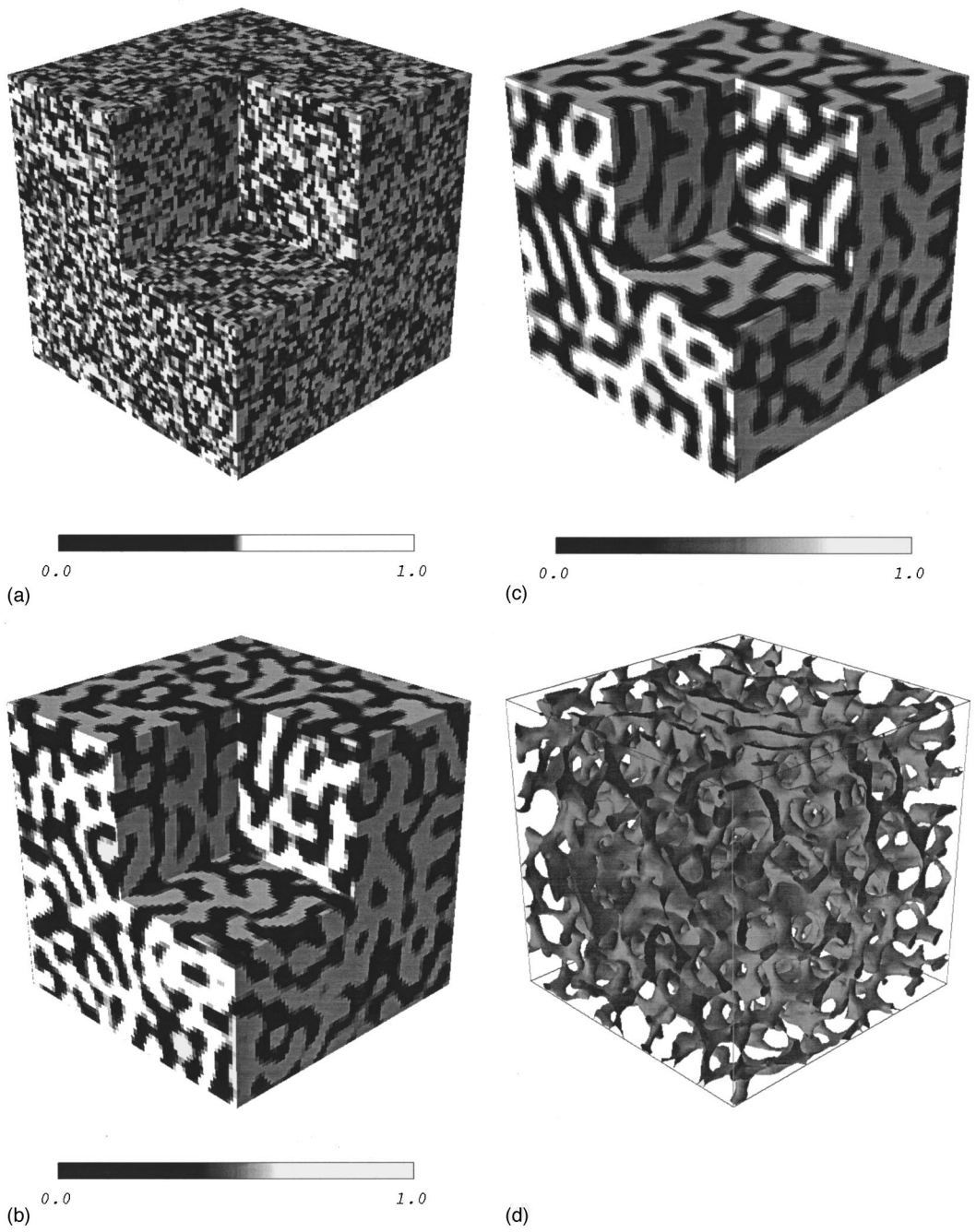

FIG. 1. Time-dependent morphology of copolymer melt A_8B_8. The melt is quenched from athermal $\chi=0$ to $\chi=1.0$ on $\tau=50$. In (a)–(c) are volume renderings of the density field $\rho_A(\mathbf{r})$ (notice that the density scale varies), in (d) is an isosurface representation of (c) (level $\rho_A=0.85$). Times: (a) $\tau=45$, (b) $\tau=125$, (c) $\tau=500$, these times correspond to the markers in Fig. 3.

estimates for ν/a^3 can be obtained from group contribution techniques[39,40] and from molecular modeling.

For some flexible polymers which are commonly used in experimental copolymer melt studies the ratio ν/a^3 can be evaluated more directly. In a recent experimental study[41] regarding the phase transitions of a poly(ethylene-propylene)-poly(ethyl-ethylene) diblock copolymer melt a chain conformation parameter β_c is introduced as $\beta_c^2=a^2/6\nu$. For this polymer β_c^2 is in the range 0.05–0.13 Å^{-1} (depending on block type) while the effective statistical length a is $\approx$7.20–7.54 Å.[41] Together, these data suggest $\nu/a^3=1/6\beta_c^2 a \approx 0.17-0.46$. This is considerably larger than the value we have used in the numerical calculations.

The relatively small ratio ν/a^3 in our study has important consequences for the value of the fluctuation corrected interaction parameter χ_e at the microphase transition. The fluctuation theory of Fredrickson and Helfand[42] predicts that

$$\chi_e N=\chi_0 N+41.0N_e^{-1/3},$$

where χ_0 is the value of χ at the microphase transition in the absence of fluctuations, this is $\chi_0 N=12.64$ for the A_8B_8 melt (the deviation from the Leibler value $\chi_0 N=10.495$ is due to

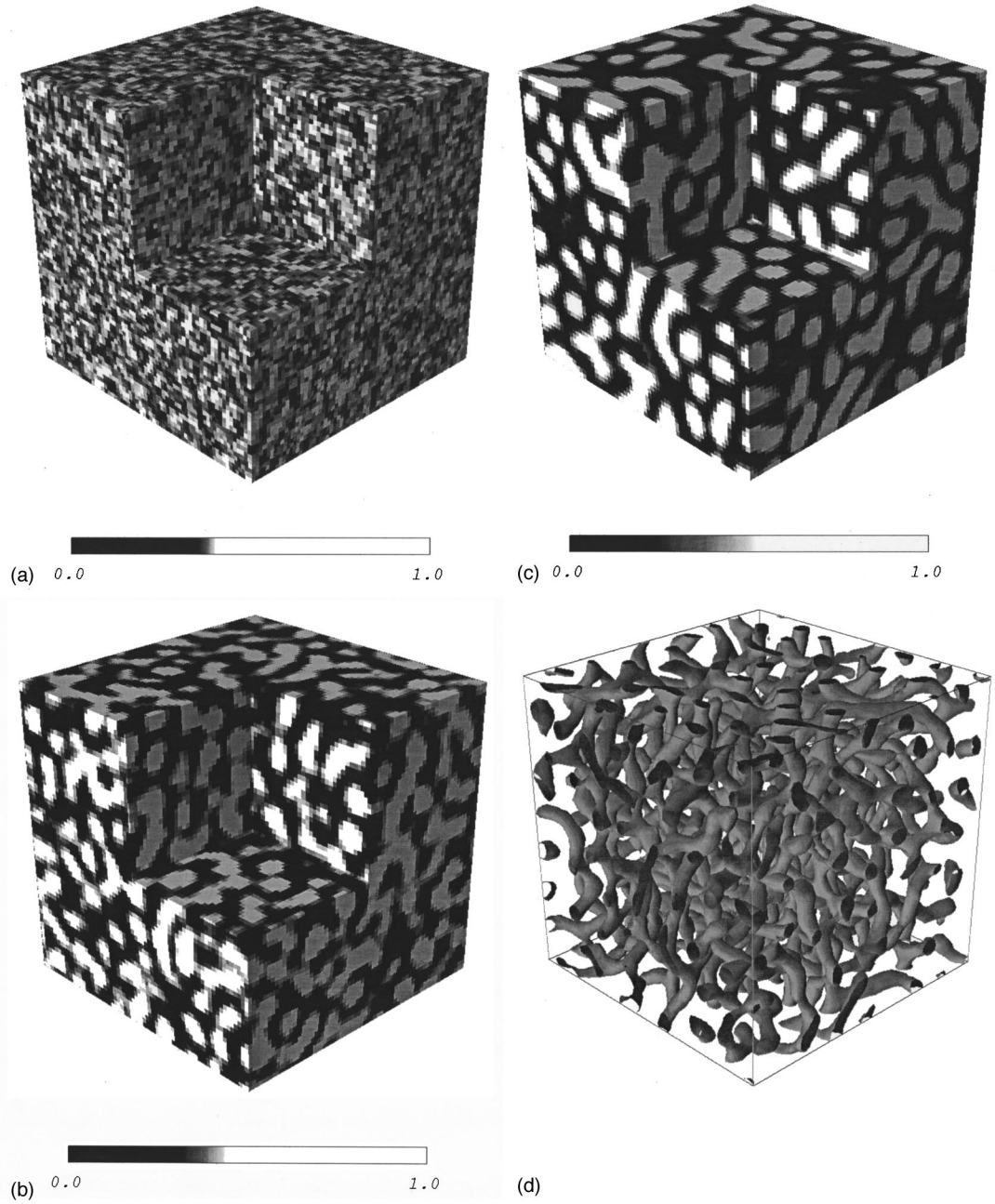

FIG. 2. Time-dependent morphology of copolymer melt A_6B_{10}. The melt is quenched from athermal $\chi=0$ to $\chi=1.0$ on $\tau=50$. In (a)–(c) are volume renderings of the density field $\rho_A(\mathbf{r})$ (notice that the density scale varies), in (d) is an isosurface representation of (c) (level $\rho_A=0.7$). Times: (a) $\tau=45$, (b) $\tau=125$, (c) $\tau=500$, these times correspond to the markers in Fig. 3.

the relatively small size of the chain and the nonlocality of the nonideal interactions—these effects are unimportant for the present argument). N_e is an effective chain length, defined as

$$N_e \equiv N a^6 \nu^{-2}.$$

In the reported simulations $N_e \approx 3.8\times 10^5$. As a result, the fluctuation correction of the interaction parameter is very small $\chi_e - \chi_0 = 1/N 41.0 N_e^{-1/3} \approx 0.035$. In a following report we will discuss these and related effects in more detail.

In several numerical experiments we tested the dynamics with larger values for ν/a^3, also using different scaling ratios d. From the results so far, it seems that simulations of practical interest can be done for $\Omega \geqslant O(5)$ and $\max(\nu/a^3) = O(0.1\text{–}0.5)$, which is in the range of the experimental polymer data.

C. Kinetic coefficients

An important point is whether local exchange is a reasonable coarse-grained kinetic mechanism for spatiotemporal collective density variations. We consider the local exchange idea the weak point in the present analysis, which needs to be improved upon in further studies. We have chosen the

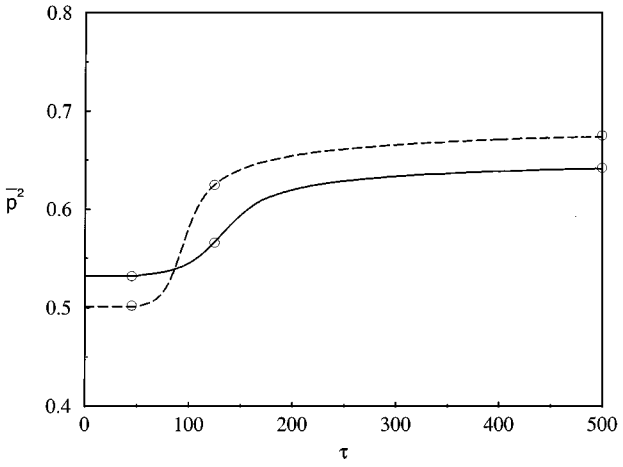

FIG. 3. Time evolution of volume-averaged order parameter $\overline{p^2}$ [for definition see Eq. (33)] for A_8B_8 (solid line) and A_6B_{10} (dashed line) copolymer melt. The markers correspond to the morphologies in Figs. 1 and 2.

local exchange form partly for computational convenience, since it is simple, does not require expensive nonlocal operators, and mimics roughly the exchange effects also in the nonlinear regime. But the assumption of locality is not rigorously correct. Some studies of kinetic coefficients in the coarse-grained limit have already been published.[43–48] Most of the discussions have focused on reptation of long chains. In case of reptation the kinetic coefficient is nonlocal with a decay-length of roughly the coil size.[47,48] Kawasaki and Sekimoto have derived an explicit formula for the kinetic coefficient which also holds in the nonlinear regime,[47,48] but unfortunately the nonlinear form seems to be too complex to be of use in simulation studies. An older prediction by Binder[43] states that in the linear regime apart from a prefactor the functional forms for the kinetic coefficients for Rouse dynamics and reptation dynamics are actually the same. In the present context, kinetic coefficients with these nonlocal forms would result in a certain averaging of the thermodynamic forces in the flux equations, thus perhaps preventing the occurrence of local defects. Since the length scale of the kinetic coefficient is at the most the coil size, we do not expect that the simulated dynamics of the collective mesoscale structures is much influenced by the precise form of the coefficient. We are currently investigating whether computationally tractable forms for nonlocal coefficients can be devised which also hold in the nonlinear regime. This work is in progress.

IV. CONCLUSION

In this paper we have introduced a new method for the numerical calculation of dynamic mesoscopic phenomena in copolymer melts in 3D. In particular, irregular morphologies seem to form preferentially in quenched melts. An important aspect of the method is the time-integration of functional Langevin equations, where the thermodynamic driving forces are obtained from a Gaussian chain molecular model. The numerical method has already been extended to more compound copolymer mixtures, including multicomponent copolymers, branched polymers, polymers with variable bead sizes, and compressible systems.[49] A weak point of the analysis is the assumed local exchange form for the kinetic coefficient, work to improve this is in progress.

ACKNOWLEDGMENTS

The work described in this paper was performed as part of the CAESAR project (Clusters of Computationally Intensive Applications for Engineering Design and Simulation on Scalable Parallel Architectures) which is funded under Contract No. ESPRIT EP8328 of the European Community. The project is a collaboration between the British Aerospace (prime partner), DASA, Odense Steel Shipyards, and BASF. We are thankful for the support by the European Community.

APPENDIX A: THE EXCHANGE LANGEVIN EQUATIONS

We first assume that for each type of bead the local flux is proportional to the local number of beads and the local thermodynamic force:

$$\mathbf{J}_I = -M\rho_I \nabla \mu_I + \tilde{\mathbf{J}}_I,$$

where $\tilde{\mathbf{J}}_I$ is a flux arising from thermal fluctuations. Together with the continuity equation

$$\frac{\partial \rho_I}{\partial t} + \nabla \cdot \mathbf{J}_I = 0,$$

we find bare functional Langevin equations of the simple diagonal form:

$$\frac{\partial \rho_I(\mathbf{r})}{\partial t} = M\nabla \cdot \rho_I \nabla \mu_I + \eta_I \tag{A1}$$

with the distribution of the noise η_I according to the fluctuation dissipation theorem:

$$\langle \eta_I(\mathbf{r},t) \rangle = 0,$$

$$\langle \eta_I(\mathbf{r},t)\, \eta_J(\mathbf{r}',t') \rangle = -2M\beta^{-1}\delta(t-t') \times \nabla_{\mathbf{r}} \cdot \delta(\mathbf{r}-\mathbf{r}')\rho_I \nabla_{\mathbf{r}'}.$$

Integration of these equations would lead to fluctuations in the total density $\rho_A(\mathbf{r},t)+\rho_B(\mathbf{r},t)$. However, since finite compressibility is not accounted for in the chosen form of the mean-field interaction potential, these fluctuations would not be very realistic. We therefore explicitly remove the fluctuations by imposing the incompressibility constraint $\nu^{-1} = \rho_A(\mathbf{r},t)+\rho_B(\mathbf{r},t)$ on the time integration. The constrained integration can be accomplished by adding an extra pressure functional to the chemical potentials, similar to the analysis in Ref. 44. The pressure functional is chosen such that any net flux of material is zero:

$$\mathbf{J}_A + \mathbf{J}_B = 0.$$

The constraining condition leads to the exchange Langevin equations in the main text, with the effective exchange ki-

netic coefficient $M\nu\rho_A\rho_B$. The application of the fluctuation dissipation theorem to the exchange equations can be found in Ref. 10.

APPENDIX B: DISCRETIZATION SCHEMES

1. Langevin equations

The Crank-Nicolson equations are

$$\theta_{Ap}^{k+1}-\omega\Delta\tau f_p^{k+1}=\theta_{Ap}^{k}+(1-\omega)\Delta\tau f_p^{k}+\eta_p^k, \tag{B1}$$

$$\theta_{Bp}^{k+1}+\omega\Delta\tau_p^{k+1}=\theta_{Bp}^{k}-(1-\omega)\Delta\tau f_p^{k}-\eta_p^k, \tag{B2}$$

$$f_p=\sum_{\alpha=1}^{m}\sum_q d_\alpha[D_\alpha\theta_A\theta_B D_\alpha]_{pq}\phi_q, \tag{B3}$$

$$\langle\eta_p^k\rangle=0, \tag{B4}$$

$$\langle\eta_p^k\eta_q^l\rangle=-2\Omega^{-1}\Delta\tau\delta_{kl}^K\sum_{\alpha=1}^{m}\sum_q d_\alpha[D_\alpha\theta_A\theta_B D_\alpha]_{pq}. \tag{B5}$$

See the main text for the definition of the parameters. The dimensionless field variables are

$$\theta_I\equiv\nu\rho_I, \tag{B6}$$

$$\phi\equiv\beta(\mu_A-\mu_B). \tag{B7}$$

The mesh size is h, k is a time increment counter, p and q are grid point counters [X_p is $X(\mathbf{r}_p)$, the value of the field X at position $\mathbf{r}_p$ on the grid], $\Delta\tau$ is the time step, ω is the Crank-Nicolson parameter ($\omega=0.5$ in the reported calculations), and D_α is a grid-restricted half-point first derivative operator in lattice direction α. We use 13 lattice directions in total (see below). The Crank-Nicolson equations are solved numerically with respect to the external potentials at time-step $k+1$ (periodic boundary conditions). Reference 10 contains a detailed discussion of the numerical calculation of the noise and the grid-restricted diffusion operator.

Notice that concerning the nonideal interactions the reduced potential ϕ can be written as a function of the χ parameter:

$$\phi(\mathbf{r})=-\beta U_A(\mathbf{r})+\beta U_B(\mathbf{r})+2\chi\left(\frac{3}{2\pi a^2}\right)^{3/2}\times\int_V e^{-(3/2a^2)(\mathbf{r}-\mathbf{r}')^2}\theta_B(\mathbf{r}')d\mathbf{r}'+\beta\nu^{-1}\left[\epsilon_{AA}^0-\frac{1}{2}(\epsilon_{AB}^0+\epsilon_{BA}^0)\right]. \tag{B8}$$

The gradient of the constant term $\beta\nu^{-1}[\epsilon_{AA}^0-1/2(\epsilon_{AB}^0+\epsilon_{BA}^0)]$ is zero and therefore omitted in the calculations.

2. Gaussian chain density functional

The discretization of the Langevin equation leaves the mesh size h unspecified. We have shown elsewhere[9] that there is an optimal value for h in terms of the Gaussian bond length parameter a. The details of the analysis are omitted here. In the numerical calculations we use the following trace over single-chain coordinates (see main text for a discussion of the normalization issue):

$$\mathrm{Tr}_c(\cdot)=\frac{1}{\Lambda^3(2\pi a^2/3)^{3/2(N-1)}}\int_{V^N}(\cdot)\prod_{s=1}^{N}d\mathbf{R}_s. \tag{B9}$$

We calculate the Gaussian chain density functional using once-integrated Green propagators.[30,29,50] We have the recursion scheme

$$G_0(\mathbf{r})=G_{N+1}^i(\mathbf{r})=1, \tag{B10}$$

$$G_s(\mathbf{r})=e^{-\beta U_s(\mathbf{r})}\sigma[G_{s-1}](\mathbf{r}), \tag{B11}$$

$$G_s^i(\mathbf{r})=e^{-\beta U_s(\mathbf{r})}\sigma[G_{s+1}^i](\mathbf{r}), \tag{B12}$$

with the Gaussian connectivity operator defined by

$$\sigma[X](\mathbf{r})\equiv\left(\frac{3}{2\pi a^2}\right)^{3/2}\int_V e^{-(3/2a^2)(\mathbf{r}-\mathbf{r}')^2}X(\mathbf{r}')d\mathbf{r}' \tag{B13}$$

with the normalization $\sigma[1](\mathbf{r})=1$. The single-chain partition function can be calculated from the propagators through

$$\Lambda^3\Phi=\int_V G_N(\mathbf{r})d\mathbf{r}=\int_V G_1^i(\mathbf{r})d\mathbf{r}. \tag{B14}$$

Expressed in terms of the Green functions the density functional is

$$\rho_I[U](\mathbf{r})=\frac{n}{\Lambda^3\Phi}\sum_{s=1}^{N}\delta_{Is}^K G_s(\mathbf{r})\sigma[G_{s+1}^i](\mathbf{r}). \tag{B15}$$

The discretization involves replacing the connectivity operator by a grid-restricted convolution, using an isotropic 27-points stencil (i.e., 13 lattice directions, another word for stencil is ''computational molecule'') with special weights. On the grid we have:[9]

$$\sigma[X](\mathbf{r}_p)=c_{000}X(\mathbf{r}_p)+\tfrac{1}{2}\sum_{\alpha=1}^{m}c_\alpha[X(\mathbf{r}_p+\mathbf{r}_\alpha)+X(\mathbf{r}_p-\mathbf{r}_\alpha)], \tag{B16}$$

where the lattice vectors $\mathbf{r}_\alpha$ are composed from the unit vectors in positive half-space. The weights c_α depend on the grid scaling ratio $d=ah^{-1}$. In Ref. 9 we have shown that isotropy and scaling conditions can be used to derive optimal values for the weights and the grid scaling:

$$c_{000}=0.171\,752,$$

$$c_{100}=0.137\,231,$$

$$c_{110}=0.054\,824\,3,$$

$$c_{111}=0.021\,902\,5,$$

$$dh^{-1}=1.154\,30.$$

It must be noted that the above stencil algorithm for the Gaussian chain density functional calculation does not place any grid restriction on the conformations of the chain. In the

physical sense the algorithm is therefore essentially off-lattice—even though we use grid-restricted operators to calculate the field values.

[1] O. T. Valls and J. E. Farrell, Phys. Rev. E **47**, R36 (1993).
[2] T. Kawakatsu, K. Kawasaki, M. Furusaka, H. Okabayashi, and T. Kanaya, J. Chem. Phys. **99**, 8200 (1993).
[3] A. Shinozaki and Y. Oono, Phys. Rev. E **48**, 2622 (1993).
[4] M. C. Cross and P. C. Hohenberg, Rev. Mod. Phys. **65**, 851 (1993).
[5] B. Schmittmann and R. K. P. Zia, *Phase Transitions and Critical Phenomena*, edited by C. Domb and J. Lebowitz (Academic, London, 1994).
[6] P. M. Chaikin and T. C. Lubensky, *Principles of Condensed Matter Physics* (Cambridge University Press, Cambridge, England, 1995), Chap. 8, pp. 464–479.
[7] P. C. Hohenberg and B. I. Halperin, Rev. Mod. Phys. **49**, 435 (1977).
[8] J. G. E. M. Fraaije, J. Chem. Phys. **99**, 9202 (1993).
[9] N. M. Maurits, P. Altevogt, O. A. Evers, and J. G. E. M. Fraaije, Comp. Polymer Sci. **6**, 1 (1996).
[10] B. A. C. Van Vlimmeren and J. G. E. M. Fraaije, Comput. Phys. Commun. **99**, 21 (1996).
[11] N. David Mermin, Phys. Rev. **137**, A1441 (1965).
[12] Frank S. Bates and Glenn H. Fredrickson, Annu. Rev. Phys. Chem. **41**, 525 (1990).
[13] Frank S. Bates, Jeffrey H. Rosedale, and Glenn H. Fredrickson, J. Chem. Phys. **10**, 6255 (1990).
[14] Ludwik Leibler, Macromolecules **13**, 1602 (1980).
[15] E. Helfand and Z. R. Wasserman, Macromolecules **9**, 879 (1976).
[16] E. Helfand and Z. R. Wasserman, Macromolecules **13**, 994 (1980).
[17] E. Helfand and Z. R. Wasserman, Macromolecules **11**, 960 (1978).
[18] P. M. Chaikin and T. C. Lubensky, *Principles of Condensed Matter Physics* (Cambridge University Press, Cambridge, England, 1995), Chap. 4, pp. 188–198.
[19] M. W. Matsen, J. Chem. Phys. **102**, 3884 (1995).
[20] M. W. Matsen and M. Schick, Phys. Rev. Lett. **72**, 2660 (1994).
[21] M. W. Matsen and M. Schick, Macromolecules **27**, 6761 (1994).
[22] M. W. Matsen and M. Schick, Macromolecules **27**, 7157 (1994).
[23] K. Binder, Adv. Polymer Sci. **112**, 181 (1994).
[24] Robert L. Lescanec and M. Muthukumar, Macromolecules **26**, 3908 (1993).
[25] M. Olvera de la Cruz and I. C. Sanchez, Macromolecules **19**, 2501 (1986).
[26] Monica Olvera de la Cruz, Phys. Rev. Lett. **67**, 85 (1991).
[27] G. H. Fredrickson and Frank S. Bates (unpublished).
[28] D. Chandler, *Introduction to Modern Statistical Mechanics* (Oxford University Press, New York, 1987).
[29] P.-G. de Gennes, *Scaling Concepts in Polymer Physics* (Cornell University Press, Ithaca, NY, 1979).
[30] M. Doi and S. F. Edwards, *The Theory of Polymer Dynamics* (Clarendon, Oxford, 1986).
[31] R. Evans, Adv. Phys. **28**, **143** (1979).
[32] J. T. Chayes and L. Chayes, J. Stat. Phys. **36**, 471 (1984).
[33] *Fundamentals of Inhomogeneous Fluids*, edited by D. Henderson (Marcel Dekker, New York, 1992).
[34] C. W. Gardiner, *Handbook of Stochastic Methods* (Springer, Berlin, 1990).
[35] H. Risken, *The Fokker-Planck Equation* (Springer, Berlin, 1989).
[36] N. G. Van Kampen, *Stochastic Processes in Physics and Chemistry* (North-Holland, Amsterdam, 1992).
[37] W. H. Press, B. P. Flannery, S. A. Teukolky, and W. T. Vetterling, *Numerical Recipes* (Cambridge University Press, Cambridge, England, 1987).
[38] Z. Xu, N. Hadjichristidis, L. J. Fetters, and J. W. Mays, Adv. Polymer Sci. **120**, 1 (1995).
[39] D. W. Krevelen, *Properties of Polymers, Their Correlation with Chemical Structure; Their Numerical Estimation and Prediction from Additive Group Contribution*, 3rd ed. (Elsevier, Amsterdam, 1990).
[40] D. Porter, *Group Interaction Modelling of Polymer Properties* (Marcel Dekker, New York, 1995).
[41] J. H. Rosedale, F. S. Bates, K. Almdal, K. Mortensen, and G. D. Wignall, Macromolecules **28**, 1429 (1995).
[42] G. H. Fredrickson and E. Helfand, J. Chem. Phys. **87**, 697 (1987).
[43] K. Binder, J. Chem. Phys. **79**, 6387 (1983).
[44] P. G. de Gennes, J. Chem. Phys. **72**, 4756 (1980).
[45] P. Pincus, J. Chem. Phys. **75**, 1996 (1981).
[46] I. Ya. Erukhmimovich and A. N. Semenov, Sov. Phys. JETP **63**, 149 (1986).
[47] K. Kawasaki and K. Sekimoto, Physica A **143**, 349 (1987).
[48] K. Kawasaki and K. Sekimoto, Physica A **148**, 361 (1988).
[49] N. M. Maurits, B. A. C. Van Vlimmeren, and J. G. E. M. Fraaije (unpublished).
[50] G. J. Fleer, M. A. Cohen Stuart, J. M. H. M. Scheutjens, T. Cosgrove, and B. Vincent, *Polymers at Interfaces* (Chapman and Hall, London, 1993).